nature ote hnology
INSIGHT| REVIEW ARTICLE
PUBLISHED ONLINE: 6 DECEMBER 2016 | DOI: 10.1038/NNANO.2010.207

The role of nanotechnology battery

Jun Lu[1], Zonghai Chen[1], Zifeng Ma[2], Feng Pan[3]*, Larry [4]* and Khalil Amine[1]*

A signi cant amount of battery research and development is underway, both in academia and industry, to meet the demand for electric vehicle applications. When it comes to designing and fabricating electrode materials, nanotechnology-based approaches have demonstrated numerous bene ts for improved energy and power density, cyclability and safety. In this Review, we o er an overview of nanostructured materials that are either already commercialized or close to commercialization for hybrid electric vehicle applications, as well as those under development with the potential to meet the requirements for long-range electric vehicles.

A battery is an electrochemical device that stores electrical energy as chemical energy in its anode and cathode during the charging process, and when needed, releases the energy as electric

marize the use of nanotechnology in other battery systems beyond Li-ion, including Li–S and Li–O_2, which we believe have the greatest potential to meet the high-energy requirement for EV applications.

Li-ion cathode materials

Since the introduction of LIBs into the market of portable electronics, the dominant cathode material has been $LiCoO_2$. However, due to its high cost and structural instability at high potential[6], this material has been ruled out as a suitable cathode material for EVs. In this section, we focus on how nanotechnology has enabled the development of other cathode materials, including olivines, doped lithium manganese oxide spinel and nickel-rich lithium-transition metal oxides.

Improving the transport properties of $LiFePO_4$. One of the rst successful alternative cathodes for automobile applications has been

edited to nanostructured $LiFePO_4$. Although this olivine has a lower energy density than $LiCoO_2$, it exhibits signi cantly higher power density, longer lifetime and improved safety. Its potential was rst recognized by John Goodenough[7], who initially suggested micrometre-sized $LiFePO_4$ for low-power applications. e low reversible capacity for micrometre-sized materials, especially at high current density, was associated with the slow movement in the Fe_xPO_4/Li_yFePO_4 ($0 < x < 0.1$, $0.9 < y < 1$) boundary during the charge/discharge cycling[7]. Attracted by its favourable electrochemical potential, low toxicity, low cost and abundance of Fe, scientists put a signi cant amount of work into understanding what hinders high-rate performances (essential in hybrid EVs (HEVs)).

It is now widely believed that the covalent character of polyanion frameworks in $LiFePO_4$ is what limits electronic conductivity. To reduce the transport length of electrons, early research mostly focused on developing nanostructured $LiFePO_4$ (refs 8, 9). To enhance the e ciency of electron injection and removal and increase performances at a high current density, nanocoating $LiFePO_4$ with a conductive medium, such as carbon[10], conductive polymer[11] or conductive metal phosphides[12,13], has also been investigated. In addition, it was shown that the electronic conductivity of nanostructured $LiFePO_4$ could be increased by a factor of ~10^8 using non-stoichiometric solid-solution doping by metal cations supervalent to Li; this discovery resulted in an olivine materials capable of being charged/discharged at an extremely high current (up to 20 °C), for complete charge/discharge of the battery in less than 3 min[14] (ref. 8).

Recent studies have also provided mechanistic insights on the Li and electronic transport mechanisms in $LiFePO_4$. Figure 1a shows the projected crystal structure of $LiFePO_4$ on the (010) direction, displaying the di usion channels for Li in the (010) direction[14]. e $[FeO_6]$ octahedrons are connected by sharing O corners to form a 2D net work in the bc plane, while the $[PO_4]$ tetrahedrons are physically separated (Fig. 1b) to connect adjunct $[Fe_1O_6]$ planes (Fig. 1c). erefore, the di usion of electrons in and out of $LiFePO_4$ relies on the $[Fe_1O_6]$ 2D framework.

Another limitation of $LiFePO_4$ is its poor percolation properties in 1D di usion channels[15]. Ab initio calculations predicted a fast-dif fusion coe cient for Li^+ in 1D channels along the (010) direction; but, the occupation of Fe ions in Li sites (anti-site defects), as commonly found in $LiFePO_4$, can prevent Li from hopping through the crystal structure. Lithium ions sitting in between a pair of defect sites are kinetically blocked (Fig. 1d, inset). Moreover, Li di usion along

[1]Chemical Sciences and Engineering Division, Argonne National Laboratory, Argonne, Illinois 60439, USA. [2]Institute of Electrochemical and Energy Technology, Department of Chemical Engineering, Shanghai Jiao Tong University, Shanghai 200240, China. [3]Materials, Peking University, Peking University Shenzhen Graduate School, Shenzhen 518055, China. [4]Material Science Division, Argonne National Laboratory, Argonne, Illinois 60439, USA. e-mail: panfeng@pkusz.edu.cn; curtiss@anl.gov; amine@anl.gov

the (001) direction is much slower and o ers a sluggish way out for the blocked lithium, resulting in high potential polarization and low rate capability[16]. Figure 1d predicts the dependence of the amount of blocked Li in the 1D channel as a function of both the percentage of defects and the length of the channel. e reduction in the particle size of $LiFePO_4$ to a critical value can substantially reduce the amount of trapped Li and reduce the e ect of the sluggish (001) di usion-channel for full utilization of the Li in the structure. As a result of these advances, nanostructured $LiFePO_4$ has been successfully deployed in HEVs and short-range EVs.

Suppressing manganese dissolution in $LiMn_2O_4$. Another class of cathode materials that has found successful applications in commercial automobiles (Chevy Volt and Nissan Leaf) is the doped lithium manganese oxide spinel, in which a percolated 3D di usion network provides an e cient removal and insertion mechanisms of Li during the charge/discharge process. One of the issues for $LiMn_2O_4$ spinel is the presence of a Jahn-Teller distortion of $[MnO_6]$ octahedrons at a low state of charge when Mn^{3+} is formed; the distortion is due to anisotropic breathing during charge/discharge cycling that results in structural instability. To mitigate the negative impact of the Jahn-Teller distortion, partial replacement of manganese with low valence state main group elements, such as lithium and aluminium, has been adopted. By reducing the amount of Mn^{3+}, this approach raises the average valence state of manganese at the end of discharge and substantially improves the cycle life of these spinels[17].

Another challenge is the dissolution of Mn^{2+} into the non-aqueous electrolyte, which eventually deposits on the surface of the graphitic anode and deteriorates the electrochemical performance[18–19]. Nanocoating with 10–20-nm-thick layers of various oxides or fluorides, such as ZrO_2 (refs 20,21), TiO_2 (refs 22,23), SiO_2 (ref. 21), Al_2O_3 (ref. 21) and AlF_3 (ref. 24) has been shown to protect the $LiMn_2O_4$ cathode from dissolution. In addition, functional electrolyte additives that form a nanopassivation layer at the electrode surface during the initial charge/discharge cycle were found to significantly improve the cycle life of this type of batteries[25–26].

Suppressing the chemical reactivity of $LiNi_{1-x-y}Mn_xCo_yO_2$. Unlike $LiCoO_2$ and $LiMn_2O_4$, in which only 0.5 Li atoms per transition metal atom deliver a reversible capacity of about 140 mAh g^{-1}, nickel-rich cathodes, $LiNi_{1-x-y}Mn_xCo_yO_2$ ($0 \leq x, y, x + y \leq 0.5$) can deliver a reversible capacity of about 200 mAh g^{-1} with an excellent capacity retention[27]. Delithiated nickel-rich cathodes are extremely reactive in non-aqueous electrolytes due to a substantial overlap between the 3*d* band of Ni and the 2*p* band of oxygen (Fig. 2)[28]. For this reason, nanoparticles and nanostructures of such cathode materials are generally undesired. Instead, nanocoatings have been used to reduce the exposed electrochemically active surface area and enhance cycle life. Nickel-rich oxides have a tendency to lose oxygen at elevated temperatures and form rock-salt NiO on the surface. is leads to a degradation of the electrochemical performance of the nal product[29]. To suppress the formation of NiO, material sintering needs to be carried out at a reduced temperature and/or oxygen-rich environment. is makes it di cult for commercial-scale synthesis of high-quality nickel-rich cathodes when the content of nickel is higher than 60%. erefore, the main interest for large-scale deployment in EVs of these cathodes is focused on $LiNi_{0.5}Mn_{0.3}Co_{0.2}O_2$ and $LiNi_{0.6}Mn_{0.2}Co_{0.2}O_2$.

e chemical reaction between the charged nickel-rich cathode and the non-aqueous electrolyte leads to substantial reduction in reversible capacity (a loss of accessible lithium), a hike in the inter

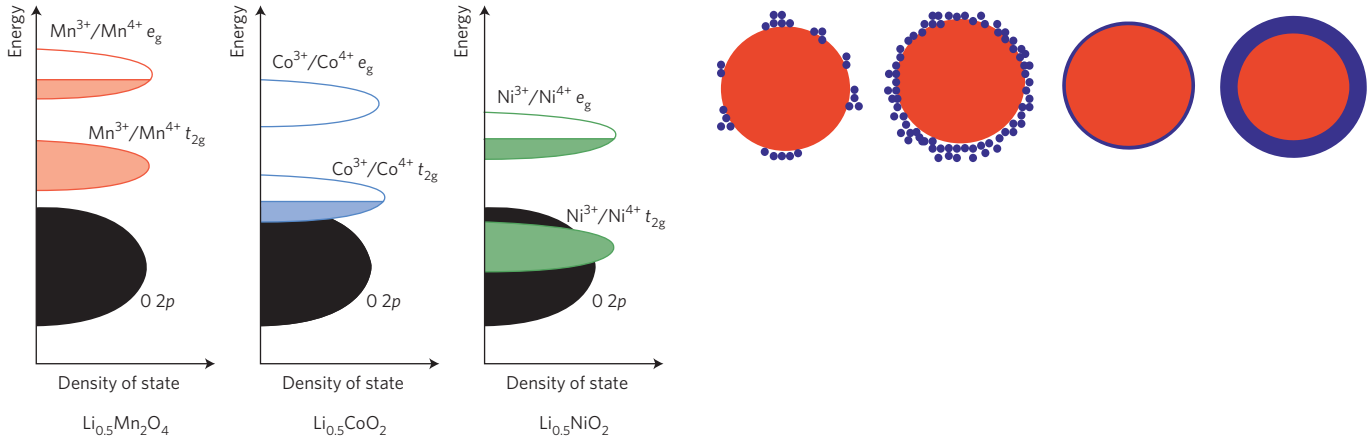

Figure 2 | **Comparison of energy** diagrams of vario In the $LiCoO_2$ system, the t_{2g} band is completely lled and the e_g band is empty ($t_{2g}^6e_g^0$) with a low-spin Co^{3+} $3d^6$ con guration. During lithium extraction, electrons are removed from the t_{2g} band rst. Since the t_{2g} band overlaps with the top of the O 2p band, deeper lithium extraction may result in a removal of electrons from the O 2p band, which will result in an oxidation of the O^{2-} ions and an ultimate loss of oxygen from the lattice. In contrast, the Li_xNiO_2 system with a low-spin Ni^{3+} $t_{2g}^6e_g^1$ con guration and the $Li_xMn_2O_4$ system with a high-spin Mn^{3+} $t_{2g}^3e_g^1$ con guration involves the removal of electrons only from the e_g band. Figure adapted from ref. 28, Elsevier.

Alternatively, a core–shell nanostructure in which a manganese-rich shell protects the high capacity nickel-rich core has been inves tigated[34] (Fig. 3d). e manganese-rich phase has a lower reversible capacity but higher chemical stability towards non-aqueous electro lytes than the nickel-rich counterpart. Although the initial cycling performance improved, long-term cycling resulted in core–shell separation due to the mismatch of the lattice parameters of the two materials. To eliminate the sudden concentration change between the core and the shell, full concentration gradient cathode materials with a nanorod structure[28] have been developed (Fig. 3e). In a typical full concentration gradient cathode, the concentration of nickel continu ously decreases from the centre towards the outer surface, while the concentration of protective material (manganese or cobalt) increases[35]. In a full cell con guration, this material can deliver a reversible spe ci c capacity of more than 200 $mAh\,g^{-1}$ and an excellent capacity retention for 1,000 cycles.

It is important to note that there is a conceptual di erence between the strategies shown in Fig. 3d,e (core–shell and full concentration gradient materials) and the development of unstructured materials. In unstructured materials (that is, without the core–shell or full concentration gradient concepts), the electrolyte can percolate into the porous structure of the particle, shortening the di usion path of lithium ions during charge/discharge, leading to a better rate capability. For the core–shell and concentration gradient materials, the percolated voids in the particle can lead to a direct exposure of the nickel-rich core towards the non-aqueous electrolyte, with a detrimental impact on both the life and safety of the battery. It is, therefore, advantageous to synthesize compact nanostructured materials that minimize the amount of voids[36]. Finally, the development of more oxidation-resistant electrolytes[37] and electrolyte additives[38–40] that can form protective nano lms on the surface of high-voltage cathodes will be bene cial for the adoption of nickel-rich cathodes for automobile applications.

Li-ion anode materials

LIB anode materials can be categorized into three groups: (1) insertion and de-insertion materials, including graphite[42] and titania[43], (2) alloy and de-alloy materials[44], such as tin and silicon alloys, and (3) conversion materials[45], such as metal oxides, metal sul des, metal uoride and metal phosphides. In this section, we focus on those materials that have been commercialized or are close to commerciali zation, especially for EV applications, and how nanotechnology has been critical in enabling the use of these materials.

Protecting graphite. Since the introduction of the rst commercial LIBs, graphite has been the anode material of choice[41,43,46,47]. Its elec trochemistry is based on the reversible intercalation/de-intercalation of Li ion into the host carbon inter-layers: $6C + xLi^+ + xe^- \rightleftharpoons Li_xC_6$ ($0 < x < 1$). e formation of LiC_6 during discharge yields a theoretical capacity of 372 $mAh\,g^{-1}$, which satis es the demand of most current portable electronic devices. e electrochemical potential of Li-ion intercalation into the graphite host lies at about 0.15– .25 V vs Li/Li, for example, making it a very attractive anode material. However, graphite also has some limitations. For instance, commonly used organic electrolytes (ethylene carbonate, diethylcarbonate, dimethylcarbonate, propylene carbonate) undergo irreversible reactions with lithiated graphite, although these electrolytes provide good conductivity[48,49]. ese side reactions include exfoliation of graphene sheets and reduction/decomposition of the electrolyte. One approach to mitigate this issue is growing a solid-electrolyte interface (SEI) as a nanosurface protection[50] by reducing ethylene carbonate molecules during the rst cycle. e SEI helps to protect the graphite and prevents electrolyte decomposition, but it is not completely e ective in passivating the

anode surface. erefore, improving protection of the graphite anode has long been actively pursued using strategies including surface oxidation[51] and protection with other nanocoatings[52].

ere are primarily three types of nanocoatings currently pursued: amorphous carbon[53–55], metal and metal oxide[56,57] and polymer[58,59]. e amorphous carbon coating is usually deposited by thermal vapour deposition (TVD) with organic precursors at a high temperature[60], or mixing graphite with polymer precursors (for example, polyvinyl chloride, PVC) and annealing the mixture at 800–1,000 °C in an argon atmosphere[61]. ese two approaches are favoured compared with chemical vapour deposition (CVD)[62,63] for large-scale industrial implementation due to lower cost. Metal and metal oxide coatings, in the order of 10–20 nm, on a graphite surface[56,57,64] e ciently minimizes side reactions with the electrolyte at the interface and improves the rate performance of the cell. ere has been a large library of materials explored for this purpose, including Cu, Ni, Sn, Zn, Al, Ag, TiO_2, MoO_3 and SnO_2 (refs 56,57,64). Many of these nanocoatings are fabricated using a wet-chemistry approach (electrolysis plating[64]), while others are applied using vacuum deposition techniques, including CVD and ALD[63]. ere are also several polymers employed for the same purpose, for instance, polyurea, polypyrrole, PVC, polyaniline and polythiophene[58,59,65–67]. All these approaches are promising for EV application considering the e ective protection of graphite they provide, as well as their potential for scale-up processing.

Improving power using nanostructured lithium titanates and titanium oxides. Lithium titanate ($Li_4Ti_5O_{12}$, LTO) spinel has proven to be a viable alternative to graphite as anode material because of its outstanding safety characteristics[68]. Li ions di use into the LTO lattice and occupy the free octahedral sites. Such insertion/de-insertion brings no strain to the host and minimum volumetric change, a very attractive property in anode materials. Moreover, the relatively high electrochemical potential of LTO for lithium insertion (~1.55 V vs Li^+/Li) renders it inert to the organic electrolyte. Most importantly, compared with graphite, LTO is an intrinsically safer anode material, with minimal irreversible capacity loss during cycling. Unfortunately, due to its unique crystal structure and large electronic bandgap (2–3 eV)[68], LTO is intrinsically limited in two aspects: (1) it has a relatively small theoretical capacity (175 mAh g^{-1}) compared with graphite (372 mAh g^{-1}) and (2) it has a low electronic and Li-ion conductivity (3×10^{-8} S cm^{-1} and 1×10^{-12}–1×10^{-13} S cm^{-1} at 300 K, respectively) compared with graphite (10^{-4} S cm^{-1} and 10^{-4}–10^{-6} S cm^{-1} at 300 K, respectively). Hence, LTO is mostly attractive for high-power applications, mainly for HEVs.

To help boost the electrochemical properties of LTO, nanotechnology has been employed in three fronts: (1) use of LTO nanostructures[69], (2) coating of LTO particle surfaces[52,70] and (3) mixing LTO nanostructures with a matrix of conductive materials[71]. Using LTO nanostructures in anodes significantly reduces the Li-ion di usion pathway within particles and also increases the exposed active electrode area to the electrolyte, both advantageous aspects to achieve high operating currents. In recent years, there have been many attempts to design e cient nanostructures (nanowires[72], nanotowers[73] and a mesoporous nest-like structure[74]) by adopting new synthetic methods or optimizing existing ones (solvothermal synthesis[75], molten-salt synthesis[76] and microwave irradiation solid-state reaction[77]). ese synthetic approaches are usually accompanied by multivalent ion doping to further increase the electronic conductivity of LTO.

Surface coating facilitates the interfacial charge transfer between the LTO and the electrolyte, enhancing the battery power density. Many of the coating materials reported for the graphite anode have also been investigated in the case of LTO, including Ag, Cu, C, SnO_2 and conductive organic compounds. Finally, processing LTO particles with conductive nanomaterials has been shown to improve the low-conductivity issue. e conductive matrix accommodates individual LTO particles, which would otherwise be insulating, providing e cient electron-transfer pathways[78] (Fig. 4).

Besides LTO, the family of TiO_2 polymorphs, including anatase, bronze (TiO_2–B), rutile and brookite phases, have also been explored as anodes for LIBs[79]. e lithium insertion/de-insertion is accompanied by the Ti $^{4+}$/Ti $^{3+}$ redox reaction: $xLi^+ + TiO_2 + xe^- \rightleftharpoons Li_xTiO_2$. Similar to LTO, the low electronic and ionic conductivities of TiO_2 prevent it from achieving superior electrochemical performance. erefore, similar nanoengineering strategies have also been widely applied for these anode materials[80]. However, it should be pointed out that commercial application of TiO_2 polymorphs in plug-in HEVs has been limited due to the relatively higher cost than LTO.

Improving energy density using silicon nanocomposites. Silicon has drawn much attention as an anode material[44,81–88] because it o ers a theoretical capacity of 3572 mAh g^{-1}, more than one order magnitude higher than graphite and LTO. Elemental Si reacts with Li via an alloy/de-alloy mechanism, forming binary Li–Si alloys. However, a volumetric change of more than 300% during battery cycling causes repeated expansion and contraction in the anode structure, leading to particle cracking and active material isolation, which ultimately results in a rapid reversible capacity loss.

In general, Si nanoparticles perform better than lms and microparticles in LIBs, because they have better tolerance to mechanical stress. erefore, several examples of Si nanostructures for anodes in LIBs have appeared in the literature[63,89,90], including 1D Si nanowires and nanotubes[91–94]. With good electronic contact between the Si nanostructures, the current collector and electrolyte, the reversible capacity of those devices can reach as high as 2,000 mAh g^{-1} with good cyclability. More complex hierarchical structures made of Si–C composites have also been reported[95], where Si nanoparticles are uniformly deposited on carbon-black dendritic backbones. In such architectures, both the Si and graphitic carbon are active components; carbon, in particular plays multiple roles: as a conductive matrix for more e cient charge transfer, as a bu er to accommodate the Si volume change and as an active Li-ion host for reversible capacity. ese structures can reach a reversible capacity of 1,950 mAh g^{-1} (ref. 96).

In terms of fabrication, CVD and other deposition techniques[97] have been used to improve the performances of Si nanostructures for LIBs. Although these studies can provide valuable insights, such vacuum deposition strategies are less applicable in large-scale commercial settings due to their high cost.

Wet-chemistry synthesis of Si–C nanocomposites provides a more realistic, low-cost alternative for industrial production[98,99]. To this end, hydro-/solvothermal preparation of Si–C nanostructures has been actively pursued, as well as supercritical- uid-liquid growth for Si nanowires[99]. By coating these Si nanowires with C, an overall reversible capacity of 1,500 mAh g^{-1} was achieved. Another alternative is the use of commercial Si nanopowder to make secondary Si–C nanostructures[100]. Si nanoparticles are encapsulated in carbon shells forming voids that allow for volume expansion during lithiation. ese carbon nanoparticles are then assembled into larger secondary microspheres (an architecture resembling a pomegranate; Fig. 5). is design not only solves the volume change issue, but also provides a stable and spatially con ned SEI between the active Si material and electrolyte, leading to very stable cycling (up to 1,000 cycles) at a speci c capacity of ~1,200 mAh g^{-1}. ough all these nanodesign e orts are worthwhile, it should be pointed out that from an engineering perspective, it may be di cult to fabricate very thin electrodes at low cost to match the thickness of the current cathode (<200 mAh g^{-1}), a drawback that could limit practical applications.

Other anode materials. ere are many other candidates that have been investigated as potential anodes for LIBs, including low-dimension carbon (graphene, carbon nanotubes and hard carbon), metal

oxides (SnO_2, Co_3O_4 and Sb_2O_3), metal nitrides ($LiMoN_2$) and metal sul des (FeS_2, NiS_2 and MoS_2). Various nanotechnologies have been actively applied in tailoring these materials for better electrochemi cal performance in LIBs. e strategies employed are overall-simi lar to what have been used in other anode materials: (1) designing nanostructures for high surface area and better lithium-ion -di u sion, (2) nanocoatings to prevent side reactions with electrolytes and (3) mixing with conductive supports to make nanocomposites with enhanced electronic conductivity. It should be noted, however, that these types of anode materials are less likely to be commercialized for EV application in the near term, mainly due to the large, irreversible capacity loss (usually between 30 and 50%) during the initial cycles.

Li–S batteries with up to 1,500 cycles have been demonstrated, they are not yet to the point of commercialization for EVs.

Conventional cathodes for Li–S batteries are made of either sulfur–carbon or sulfur–polymer composites, where the carbon or polymer are added to enhance electronic conductivity and utilization of active materials. Approaches based on nanoporous architectures have been used to immobilize lithiumot yaous arc13(o) (h)3(a)9(.9(e)2.1(so1(n)-5(h)3-11.9( )(, t)s h)45(o)12(f c)-1(o8.n <</Lang (e1()-9(o)7.1

Received 27 January 2016; accepted 12 September 2016; published online 6 December 2016

References

1. Dunn, B., Kamath, H. & Tarascon, J. M. Electrical energy storage for the grid: a battery of choices. *Science* 334, 928–935 (2011).
2. Etacheri, V., Marom, R., Elazari, R., Salitra, G. & Aurbach, D. Challenges in the development of advanced Li-ion batteries: a review. *Energy. Environ. Sci.* 4, 3243–3262 (2011).
3. Goodenough, J. B. & Park, K.-S. The Li-ion rechargeable battery: a perspective. *J. Am. Chem. Soc.* 135, 1167–1176 (2013).
4. Bruce, P. G., Freunberger, S. A., Hardwick, L. J. & Tarascon, J.-M. Li–O$_2$ and Li–S batteries with high energy storage. *Nat. Mater.* 11, 19–29 (2012).
5. Lu, J. *et al.* Aprotic and aqueous Li–O$_2$ batteries. *Chem. Rev.* 114, 5611–5640 (2014).
6. Chen, Z., Lu, Z. & Dahn, J. R. Staging phase transitions in Li$_x$CoO$_2$. *J. Electrochem. Soc.* 149, A1604–A1609 (2002).
7. Padhi, A. K., Nanjundaswamy, K. S. & Goodenough, J. B. Phospho-olivines as positive-electrode materials for rechargeable lithium batteries. *J. Electrochem. Soc.* 144, 1188–1194 (1997).
8. Chung, S. Y., Bloking, J. T. & Chiang, Y. M. Electronically conductive phospho-olivines as lithium storage electrodes. *Nat. Mater.* 1, 123–128 (2002).
9. Malik, R., Zhou, F. & Ceder, G. Kinetics of non-equilibrium lithium incorporation in LiFePO$_4$. *Nat. Mater.* 10, 587–590 (2011).
10. Zhang, K. *et al.* Conformal coating strategy comprising N-doped carbon and conventional graphene for achieving ultrahigh power and cyclability of Li$_4$FePO$_4$. *Nano Lett.* 15, 6756–6763 (2015).
11. Lepage, D., Michot, C., Liang, G., Gauthier, M. & Schougaard, S. B. A soft chemistry approach to coating of LiFePO$_4$ with a conducting polymer. *Angew. Chem. Int. Ed.* 50, 6884–6887 (2011).
12. Hu, C. *et al.* Suppressing Li$_3$PO$_4$ impurity formation in LiFePO$_4$/Fe$_2$P by a nonstoichiometry synthesis and its effect on electrochemical properties. *Mater. Lett.* 65, 1323–1326 (2011).
13. Herle, P. S., Ellis, B., Coombs, N. & Nazar, L. F. Nano-network electronic conduction in iron and nickel olivine phosphates. *Nat. Mater.* 3, 147–152 (2004).
14. Zhang, P. X. *et al.* First-principles study on the electronic structure of a LiFePO$_4$ (010) surface adsorbed with carbon. *J. Alloys Compd.* 540, 121–126 (2012).
15. Nishimura, S.-I. *et al.* Experimental visualization of lithium diffusion in Li$_x$FePO$_4$. *Nat. Mater.* 7, 707–711 (2008).
16. Malik, R., Burch, D., Bazant, M. & Ceder, G. Particle size dependence of the ionic diffusivity. *Nano Lett.* 10, 4123–4127 (2010).
17. Yuan, A., Tian, L., Xu, W. & Wang, Y. Al-doped spinel Li$_{1.04}$Mn$_{1.9}$O$_4$ with improved high-rate cyclability in aqueous electrolyte. *J. Power Sources* 195, 5032–5038 (2010).
18. Shkrob, I. A. *et al.* Manganese in graphite anode and capacity fade in Li ion batteries. *J. Phys. Chem. C* 118, 24335–24348 (2014).
19. Kumagai, N., Komaba, S., Kataoka, Y. & Koyanagi, M. Electrochemical behavior of graphite electrode for lithium ion batteries in Mn and Co additive electrolytes. *Chem. Lett.* 29, 1154–1155 (2000).
20. Lin, Y.-M. *et al.* Enhanced high-rate cycling stability of Li$_2$MO$_4$ cathode by ZrO$_2$ coating for Li-ion battery. *J. Electrochem. Soc.* 152, A1526–A1532 (2005).
21. Kim, J.-S. *et al.* The electrochemical stability of spinel electrodes coated with ZrO$_2$, Al$_2$O$_3$, and SiO$_2$ from colloidal suspensions. *J. Electrochem. Soc.* 151, A1755–A1761 (2004).
22. Lu, J. *et al.* Effectively suppressing dissolution of manganese from spinel lithium manganate via a nanoscale surface-doping approach. *Nat. Commun.* 5, 5693 (2014).
23. Yao, J., Shen, C., Zhang, P., Gregory, D. & Wang, L. Surface coating of LiMn$_2$O$_4$ spinel via in situ hydrolysis route: effect of the solution. *Ionics* 19, 739–745 (2013).
24. Liu, Y., Lv, J., Fei, Y., Huo, X. & Zhu, Y. Improvement of storage performance of LiMn$_2$O$_4$/graphite battery with AlF$_3$-coated LiMn$_2$O$_4$. *Ionics* 19, 1241–1246 (2013).
25. Komaba, S. *et al.* Impact of 2-vinylpyridine as electrolyte additive on surface and electrochemistry of graphite for C/LiMn$_2$O$_4$ Li-ion cells. *J. Electrochem. Soc.* 152, A937–A946 (2005).
26. Zhan, C., Qiu, X., Lu, J. & Amine, K. Tuning the Mn deposition on the anode to improve the cycle performance of the Mn-based lithium ion battery. *Adv. Mater. Interfaces* 3, 1500856 (2016).
27. Sun, Y.-K. *et al.* The role of AlF$_3$ coatings in improving electrochemical cycling of Li-enriched nickel-manganese oxide electrodes for Li-ion batteries. *Adv. Mater.* 24, 1192–1196 (2012).
28. Chebiam, R. V., Kannan, A. M., Prado, F. & Manthiram, A. Comparison of the chemical stability of the high energy density cathodes of lithium-ion batteries. *Electrochem. Commun.* 3, 624–627 (2001).
29. Liu, L. & Chen, X. Titanium dioxide nanomaterials: self-structural modifications. *Chem. Rev.* 114, 9890–9918 (2014).
30. Chen, Z., Qin, Y., Amine, K. & Sun, Y. K. Role of surface coating on cathode materials for lithium-ion batteries. *J. Mater. Chem.* 20, 7606–7612 (2010).
31. Cho, J., Kim, Y. W., Kim, B., Lee, J. G. & Park, B. A breakthrough in the safety of lithium secondary batteries by coating the cathode material with AlPO$_4$ nanoparticles. *Angew. Chem. Int. Ed.* 42, 1618–1621 (2003).
32. Chen, Z. & Dahn, J. R. Methods to obtain excellent capacity retention in LiCoO$_2$ cycled to 4.5 V. *Electrochim. Acta* 49, 1079–1090 (2004).
33. Meng, X., Yang, X.-Q. & Sun, X. Emerging applications of atomic layer deposition for lithium-ion battery studies. *Adv. Mater.* 24, 3589–3615 (2012).
34. Sun, Y.-K., Myung, S.-T., Kim, M.-H., Prakash, J. & Amine, K. Synthesis and characterization of Li[(Ni$_{0.8}$Co$_{0.1}$Mn$_{0.1}$)$_{0.8}$(Ni$_{0.5}$Mn$_{0.5}$)$_{0.2}$]O$_2$ with the microscale core–shell structure as the positive electrode material for lithium batteries. *J. Am. Chem. Soc.* 127, 13411–13418 (2005).
35. Sun, Y. K. *et al.* Nanostructured high-energy cathode materials for advanced lithium batteries. *Nat. Mater.* 11, 942–947 (2012).
36. Noh, H.-J. *et al.* Cathode material with nanorod structure — an application for advanced high-energy and safe lithium batteries. *Chem. Mater.* 25, 2109–2115 (2013).
37. Xu, M. *et al.* Tris (pentafluorophenyl) phosphine: an electrolyte additive for high voltage Li-ion batteries. *Electrochem. Commun.* 18, 123–126 (2012).
38. Abe, K., Ushigoe, Y., Yoshitake, H. & Yoshio, M. Functional electrolytes: novel type additives for cathode materials, providing high cycleability performance. *J. Power Sources* 153, 328–335 (2006).
39. Tarnopolskiy, V. *et al.* Beneficial influence of succinic anhydride as electrolyte additive on the self-discharge of 5 V Li$_{0.4}$Mn$_{1.6}$O$_4$ cathodes. *J. Power Sources* 236, 39–46 (2013).
40. von Cresce, A. & Xu, K. Electrolyte additive in support of 5 V Li ion chemistry. *J. Electrochem. Soc.* 158, A337–A342 (2011).
41. Winter, M., Besenhard, J. O., Spahr, M. E. & Novák, P. Insertion electrode materials for rechargeable lithium batteries. *Adv. Mater.* 10, 725–763 (1998).
42. Dahn, J. *et al.* in Lithium Batteries: New Materials, Developments, and Perspectives (ed. Pistoria, G.) Ch. 1 (Elsevier, 1994).
43. Ohzuku, T., Ueda, A. & Yamamoto, N. Zero-strain insertion material of Li[Li$_{1/3}$Ti$_{5/3}$]O$_4$ for rechargeable lithium cells. *J. Electrochem. Soc.* 142, 1431–1435 (1995).
44. Park, C.-M., Kim, J.-H., Kim, H. & Sohn, H.-J. Li-alloy based anode materials for Li secondary batteries. *Chem. Soc. Rev.* 39, 3115–3141 (2010).
45. Reddy, M., Subba Rao, G. & Chowdari, B. Metal oxides and oxysalts as anode materials for Li ion batteries. *Chem. Rev.* 113, 5364–5457 (2013).
46. Endo, M., Kim, C., Nishimura, K., Fujino, T. & Miyashita, K. Recent development of carbon materials for Li ion batteries. *Carbon* 38, 183–197 (2000).
47. Buqa, H., Goers, D., Holzapfel, M., Spahr, M. E. & Novák, P. High rate capability of graphite negative electrodes for lithium-ion batteries. *J. Electrochem. Soc.* 152, A474–A481 (2005).

61. Nozaki, H., Nagaoka, K., Hoshi, K., Ohta, N. & Inagaki, M. Carbon-coated graphite for anode of lithium ion rechargeable batteries: carbon coating conditions and precursors. J. Power Sources 194, 486–493 (2009).
62. Ding, Y.-S. et al. Characteristics of graphite anode modified by CVD carbon coating. Surf. Coat. Technol. 200, 3041–3048 (2006).
63. Lee, M.-J. et al. Atomic layer deposition of TiO_2 on negative electrode for lithium ion batteries. J. Power Sources 244, 410–416 (2013).
64. Lu, W., Donepudi, V. S., Prakash, J., Liu, J. & Amine, K. Electrochemical and thermal behavior of copper coated type MAG-20 natural graphite. Electrochim. Acta 47, 1601–1606 (2002).
65. Pan, Q., Guo, K., Wang, L. & Fang, S. Novel modified graphite as anode material for lithium-ion batteries. J. Electrochem. Soc. 149, A1218–A1223 (2002).
66. Veeraraghavan, B., Paul, J., Haran, B. & Popov, B. Study of polypyrrole graphite composite as anode material for secondary lithium-ion batteries. J. Power Sources 109, 377–387 (2002).
67. Zhang, H.-L., Li, F., Liu, C. & Cheng, H.-M. Poly(vinyl chloride) (PVC) coated ideas revisited: influence of carbonization procedures on PVC-coated natural graphite as anode materials for lithium ion batteries. J. Phys. Chem. C 112, 7767–7772 (2008).
68. Ouyang, C. Y., Zhong, Z. Y. & Lei, M. S. Ab initio studies of structural and electronic properties of $Li_4Ti_5O_{12}$ spinel. Electrochem. Commun. 9, 1107–1112 (2007).
69. Prakash, A. S. et al. Solution-combustion synthesized nanocrystalline $Li_4Ti_5O_{12}$ as high-rate performance Li-ion battery anode. Chem. Mater. 22, 2857–2863 (2010).
70. Rahman, M. M., Wang, J.-Z., Hassan, M. F., Wexler, D. & Liu, H. K. Amorphous carbon coated high grain boundary density dual phase $Li_4Ti_5O_{12}$-TiO_2: a nanocomposite anode material for Li-ion batteries. Adv. Energy Mater. 1, 212–220 (2011).
71. Kim, H.-K., Bak, S.-M. & Kim, K.-B. $Li_4Ti_5O_{12}$/reduced graphite oxide nano-hybrid material for high rate lithium-ion batteries. Electrochem. Commun. 12, 1768–1771 (2010).
72. Shen, L., Uchaker, E., Zhang, X. & Cao, G. Hydrogenated $Li_4Ti_5O_{12}$ nanowire arrays for high rate lithium ion batteries. Adv. Mater. 24, 6502–6506 (2012).
73. Chiu, H.-c. & Demopoulos, G. P. A novel green approach to synthesis of nanostructured $Li_4Ti_5O_{12}$ anode material. ECS Trans. 50, 119–126 (2013).
74. Chen, J., Yang, L., Fang, S., Hirano, S.-i. & Tachibana, K. Synthesis of hierarchical mesoporous nest-like $Li_4Ti_5O_{12}$ for high-rate lithium ion batteries. J. Power Sources 200, 59–66 (2012).
75. Laumann, A. et al. Rapid green continuous flow supercritical synthesis of high performance $Li_4Ti_5O_{12}$ nanocrystals for Li ion battery application. J. Electrochem. Soc. 159, A166–A171 (2011).
76. Bai, Y., Wang, F., Wu, F., Wu, C. & Bao, L.-y. Influence of composite LiCl–KCl molten salt on microstructure and electrochemical performance of spinel $Li_4Ti_5O_{12}$. Electrochim. Acta 54, 322–327 (2008).
77. Li, J., Jin, Y.-L., Zhang, X.-G. & Yang, H. Microwave solid-state synthesis of spinel $Li_4Ti_5O_{12}$ nanocrystallites as anode material for lithium-ion batteries. Solid State Ion. 178, 1590–1594 (2007).
78. Shen, L. et al. Free-dimensional coherent titania 56 >6 BT476an <ala(Ab f)9-5(a)n 2142 >>BDC BT -0.014 Tc 0.014 Tw 7.5 0 0 7.5 5578.